Aerobic oxidation of benzyl alcohol in a slug flow microreactor

Hommes, Arne; Disselhorst, Bas; Yue, Jun

Published in:
AIChE Journal

DOI:
10.1002/aic.17005

Publication date:
2020

Received: 6 September 2019 | Revised: 13 May 2020 | Accepted: 3 August 2020

DOI: 10.1002/aic.17005

REACTION ENGINEERING, KINETICS AND CATALYSIS

AIChE JOURNAL

Aerobic oxidation of benzyl alcohol in a slug flow microreactor: Influence of liquid film wetting on mass transfer

Arne Hommes | Bas Disselhorst | Jun Yue

Department of Chemical Engineering, Engineering and Technology Institute Groningen, University of Groningen, Groningen, The Netherlands

Correspondence
Jun Yue, Department of Chemical Engineering, Engineering and Technology Institute Groningen, University of Groningen, Nijenborgh 4, 9747 AG Groningen, The Netherlands.
Email: yue.jun@rug.nl

Funding information
Rijksuniversiteit Groningen, Grant/Award Number: Not applicable; University of Groningen

Abstract

Homogeneous Co/Mn/Br catalyzed aerobic oxidation of benzyl alcohol in acetic acid to benzaldehyde was performed in polytetrafluoroethylene microreactors operated under slug flow at temperatures up to 150°C and pressures up to 5 bar. Depending on the bubble velocity and length, a wetted or dewetted slug flow was observed, characterized typically by a complete or partially wetting liquid film around the bubble body. The latter flow suffered from a limited interfacial area for mass transfer. Experiments at temperatures up to ca. 90°C were under kinetic control given no product yield difference under wetted and dewetted slug flows and were used to establish a simplified kinetic expression (first order in benzyl alcohol and zero order in oxygen). This allows to develop a mass transfer model combined with an instantaneous reaction regime that well described the experimental results at higher temperatures where mass transfer was limiting in the dewetted slug flow.

KEYWORDS

benzyl alcohol oxidation, mass transfer, microreactor, slug flow, wettability

1 | INTRODUCTION

Oxidation reactions are important for the industrial production of alcohols, aldehydes and carboxylic acids from hydrocarbons.[1] A big challenge thereof is to prevent the over-oxidation and other unwanted side reactions, requiring highly active and selective catalysts (e.g., the often used transition metals).[2] The oxidation of *p*-xylene to terephthalic acid, a monomer for producing polyethylene terephthalate (PET), is industrially performed in the Amoco Mid-Century (MC) process using metal bromide (Co/Mn/Br) complexes as homogeneous catalyst with acetic acid as the solvent.[3] This oxidation reaction proceeds via a free-radical chain mechanism. Herein, Co(III), formed via the Haber–Weiss cycle, and a bromide ion react to generate a bromine radical. This radical subsequently initiates the oxidation of hydrocarbons to form an alcohol, aldehyde or carboxylic acid.[4] The performance of metal bromide complexes for the oxidation of *p*-xylene and other hydrocarbons (e.g., toluene to benzaldehyde and benzoic acid) has been researched extensively.[3-7] The conversion of alcohols using these catalytic systems has been examined to a lesser extent; however, it is generally accepted that these proceed via similar mechanisms.[8,9] Typically, the benzyl alcohol oxidation to benzaldehyde and benzoic acid has been investigated with Co/Mn/Br complexes in acetic acid (Scheme 1) in semi-batch reactors operated under atmospheric pressure and temperatures between 75°C and 95°C.[8,9] Air was fed through a frit at the bottom of the reactor, resulting in an upward bubbly flow.

Traces of benzyl acetate (maximum about 5% yield) are formed as an intermediate by the esterification of benzyl alcohol and the acetic acid (AcOH) solvent, which can further oxidize to benzaldehyde. The oxidation of benzyl alcohol appears very selective toward benzaldehyde and (eventually) benzoic acid, practically without the over-oxidation to CO and CO_2.[8] Interestingly, the presence of benzyl alcohol inhibits the formation of benzoic acid from benzaldehyde,[9,10] because benzyl alcohol intercepts the (benzoylperoxy) radicals that

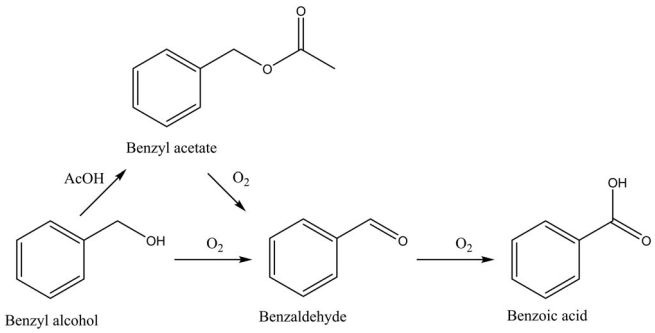

SCHEME 1 Aerobic oxidation of benzyl alcohol to benzaldehyde and benzoic acid over metal bromide catalysts in the acetic acid solvent with benzyl acetate as a possible intermediate

induce the further oxidation toward benzoic acid. Therefore, only at low benzyl alcohol concentrations, the further oxidation of benzaldehyde toward benzoic acid occurs significantly. This makes the metal bromide catalyzed oxidation of benzyl alcohol an attractive route for the selective synthesis of benzaldehyde as compared to the industrial route by the gas phase oxidation of toluene (where the majority of toluene is converted to benzoic acid).[5,6] Benzaldehyde finds its application in flavorings, fragrances, and cosmetics or as a precursor for producing pharmaceuticals and plastic additives.[11] Metal bromide catalysts have also shown to effectively catalyze the oxidation of other industrially relevant compounds. Some studies reported the oxidation of 5-hydroxymethylfurfural (HMF), a promising biobased platform chemical derived from sugars,[12] with Co/Mn/Br catalyst in acetic acid.[8,13,14] These were performed in a semi-batch reactor with an upward bubbly flow at atmospheric pressure,[8] or in (fed-)batch autoclaves under elevated pressures/temperatures with a gas-inducing impeller by which oxygen bubbles were generated in the liquid phase through a sparger.[13,14] This resulted in 2,5-diformylfuran (DFF) and 2,5-furandicarboxylic acid (FDCA) that find potential applications in, for example, resins, pharmaceuticals, or as polymer building blocks.[15] In a fed-batch reactor operated at elevated pressures and temperatures, the FDCA formation rate was limited by the gas–liquid mass transfer as shown by the notable influence of stirring rate on the reaction performance.[14] Also the oxidation of lignin, a major polymeric component in biomass, was performed with Co/Mn/Zr/Br catalysts in acetic acid.[16] A total yield of 10.9% toward value-added oxidation products (vanillin, vanillic acid, syringaldehyde, and syringic acid) was obtained, which is in a similar value range to other catalytic systems.[17] For an effective and selective retrieval of lignin oxidation products, dedicated studies on separation strategies should be performed.

Microreactors represent a promising process intensification tool for gas–liquid (oxidation) reactions.[18-20] They consist of mainly capillary- or chip-based channels with a typical inner diameter on the order of ca. 1 mm or below. Due to the small internal channel sizes, microreactors offer a larger surface area to volume ratio than conventional reactors, and consequently several fundamental advantages such as the enhanced heat and mass transfer. Thus, gas–liquid flow processing in microreactors allows to intensify reactions with fast kinetics that are often limited by interfacial mass transfer. Well-defined gas–liquid (e.g., slug or annular) flow patterns in microreactors enable a precise tuning of the interfacial area and mass transfer for controlled chemical synthesis and obtaining valuable kinetic insights.[21,22] Besides, for liquid phase oxidation reactions that are often highly exothermic, heat transfer intensification in microreactors enables a tight temperature control for improved process performance. Also, explosive risks (e.g., when using pure oxygen) can be handled with ease in microreactors. Hence, liquid phase oxidation reactions using molecular oxygen as the oxidant have been widely performed in microreactors.[23,24] Although the aerobic oxidation of benzyl alcohol to benzaldehyde was often researched over heterogeneous catalysts in (packed bed) microreactors,[25-27] there seems to be only one report related to the use of homogeneous catalysis in a microreactor.[28] This was conducted under slug flow in a perfluoroalkoxy alkane capillary with an inner diameter (d_C) of 1.6 mm using a Cu/TEMPO catalyst in acetonitrile.[28] Herein, 70% benzyl alcohol conversion was obtained in 5 min at room temperature and 5 bar oxygen, which was considerably faster than in conventional (stirred batch) reactors where it took several hours to obtain the same results. Such enhanced reaction rate is due to the significant mass transfer increase in the microreactor. Despite this, the use of Cu/TEMPO catalyst on a large scale may not be feasible given its high cost. In this respect, cheaper homogeneous catalysts (e.g., metal bromides) are more favored in the industry.

In this work, the homogeneous Co/Mn/Br catalyzed oxidation of benzyl alcohol to benzaldehyde using acetic acid as the solvent and air or pure oxygen as the oxidant was studied in capillary microreactors made of polytetrafluoroethylene (PTFE) operated under a gas–liquid slug flow. Due to the marginal wettability of acetic acid on PTFE,[29] a wetted or dewetted slug flow was observed in the microreactor depending on the bubble length and velocity therein. The dewetted slug flow (also referred to as a [dry] plug flow) is typically characterized by a (partial) absence of liquid film surrounding the bubble.[30-32] Under such flow profile, a typically lower specific surface area is obtained in the microreactor, which decreases the multiphase mass transfer rate therein.[33,34] Despite this, there are some advantages over the wetted slug flow for certain applications. Under a dewetted slug flow, the slug-to-slug interaction is further reduced due to the (partial) absence of liquid film, resulting in a narrower liquid phase residence time distribution.[35] This may be advantageous for studies in which a proper tuning of concentration distributions of substrate/product is required.

The microreactor in this work was operated at temperatures up to 150°C and pressures up to 5 bar. Flow conditions were varied at relatively low and elevated temperatures to identify under which conditions the reaction rate was limited by kinetics or mass transfer, aided by analyzing the influence of the wetting behavior of the liquid film around bubbles on mass transfer. The substrate and catalyst concentrations, partial oxygen pressure and temperature were varied to obtain a simplified kinetic expression at low temperatures (up to ca. 90°C). This expression was subsequently used to develop a mass transfer model describing the reaction results at higher temperatures

where mass transfer appeared limiting in slug flow with the dewetted liquid films. This work provides important guidelines to further optimize the Co/Mn/Br catalyzed oxidation of benzyl alcohol (as well as other aromatic alcohols) and additional insights regarding the influence of liquid film wetting behavior on mass transfer under gas–liquid slug flow in microreactors.

2 | EXPERIMENTAL

2.1 | Chemicals

Benzyl alcohol (≥99.0%), benzaldehyde (≥99.0%), benzoic acid (≥99.5%), benzyl acetate (≥99.0%), pentadecane (≥98.0%), manganese(II) acetate tetrahydrate (≥99.0%), cobalt(II) acetate tetrahydrate (reagent grade), and NaBr (≥99.0%) were obtained from Sigma-Aldrich. Acetic acid (≥ 99.5%) was purchased from Acros and acetone (≥ 99.8%) from Biosolve. Compressed air and oxygen were obtained from Linde gas.

2.2 | Setup

Figure 1 presents a schematic overview of the microreactor setup. The flow rate of air or oxygen ($Q_{G,0}$ = 0.5–2.0 mL/min) fed from the cylinder was controlled by a mass flow controller (MFC; Bronkhorst High-Tech model F-200 CV). To stablize the gas–liquid flow in the microreactor, a small-diameter polyether ether ketone (PEEK) capillary (inner diameter: 50 μm; length: 15 cm) was installed in the gas flow route as the flow restrictor in order to create a large pressure barrier before the gas reached the inlet T-junction (made of PEEK; inner diameter: 0.2 mm). The flow rate of liquid mixture that contained the substrate and catalyst in acetic acid ($Q_{L,0}$ = 0.1–0.4 mL/min) was adjusted by an HPLC pump (Hewlett Packard Agilent series 1100). Upon mixing in the T-junction, a gas–liquid slug flow was generated in the connecting PTFE capillary microreactor heated in an oil bath. Microreactors of different inner diameters (d_C = 0.5, 0.8, or 1.0 mm) and effective lengths (L_C = 0.4–10-m; i.e., of the section immersed in the oil bath) were used. The reaction occurrence was expected negligible both in the short microreactor section (ca. 10 cm in length) before the oil bath (i.e., at room temperature) and that after the bath (length of ca. 20–30 cm; given a rapid cooling of the reaction mixture to near room temperature due to primarily the large surface to volume ratio of the microreactor and the strong ventilation around the setup that was positioned in a fume hood; calculation details not shown for brevity). For experiments conducted under atmospheric pressure conditions, the temperature (T) was varied from 70 to 90°C and the microreactor outlet was open to air. For experiments at elevated pressures (5 bar; T = 90–150°C), a compact spring-loaded, diaphragm-operated back pressure regulator (BPR) from Porter (Model 9000) was used to control the pressure at the gas outlet (Figure 1). This BPR was operated similarly to a pressure relief valve, where the desired pressure was set manually. Pressures in the gas line right before the flow restrictor and BPR (if present) were monitored with digital pressure indicators (PIs) from ESI-TEC (Model GS4200-USB). From the measured pressures at the microreactor in- and outlet, the pressure drop under gas–liquid slug flow was determined to be in a range of 0.02–0.4 bar, depending on the microreactor length and inner diameter, mixture velocity, and slug flow profile involved. Slug flow pictures in the microreactor were captured with a Nikon D3300 digital camera, equipped with a Nikon lens (AF-S Micro Nikkor 60 mm f/2.8 G ED), using an LED illuminator (Fiber-Lite MI-LED A2) from Dolan-Jenner Industries as the backlight.

2.3 | Reaction test procedure

The catalyst mixture was prepared by dissolving $Co(OAc)_2$, $Mn(OAc)_2$ and NaBr, in acetic acid at a cobalt concentration (C_{Co}) of 2–45 mM.

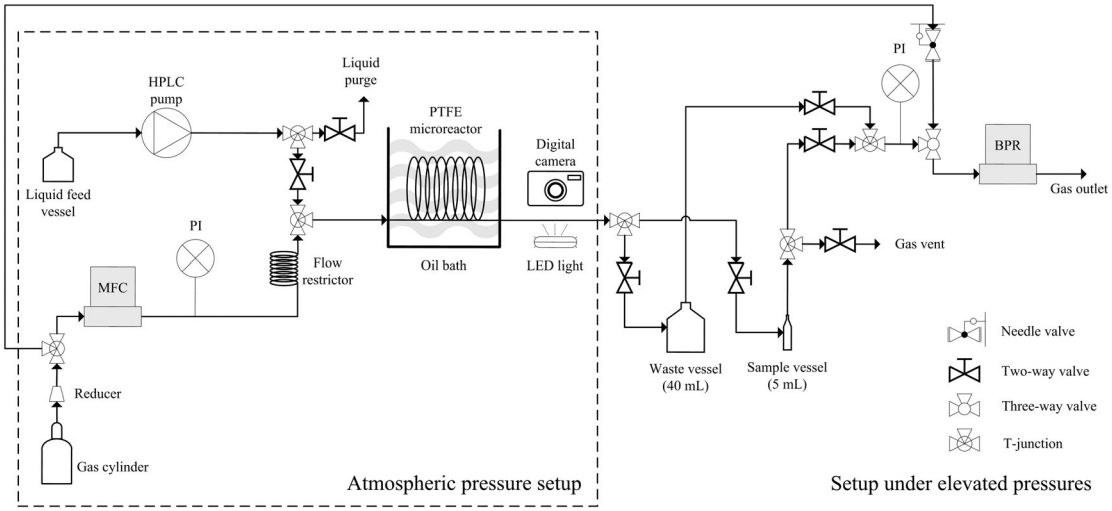

FIGURE 1 Schematic representation of the microreactor setup. The dashed box indicates operation under atmospheric pressure conditions

For all the experiments, the molar catalyst composition is Co/Mn/Br = 1/1/3.3. NaBr was used instead of HBr to minimize corrosion of the reactor equipment.[3,4] Then, benzyl alcohol was added to the mixture (in a concentration range of 85–365 mM) for use as the liquid feed. For experiments conducted at atmospheric pressure conditions (Figure 1), the microreactor outlet was directed to a sample vial, where the liquid phase was collected, and the gas phase was exhausted to the atmosphere. Most experiments were performed at 90°C (i.e., to prevent solvent evaporation and maintain a stable and uniform slug flow profile) and an initial gas to liquid flow ratio ($Q_{G,0}/Q_{L,0}$) of 5. At this ratio, there was no shortage of oxygen in the microreactor (cf. section S1) and bubbles were not so long as to negatively affect the liquid residence time distribution and slug flow profile (vide infra). At least two liquid samples were taken under the steady-state conditions to ensure a good experimental reproducibility. For experiments under elevated pressure conditions, the setup was prepressurized with air up to 5 bar before the liquid flow was introduced. Gas was continuously exhausted through the BPR and the liquid outlet was collected in a waste vessel until the gas–liquid slug flow was stable and no pressure alterations were observed. The liquid outlet was then redirected to a sample tank after waiting for at least four times the residence time under the stabilized flow conditions. Once a sufficient liquid sample was collected, the flow was directed to the waste vessel again so that the sample vessel could be depressurized and removed safely. All pressurized experiments were performed at least in duplicate. In addition, photographs of the gas–liquid flow pattern at the microreactor outlet (and occasionally at the inlet) were taken at representative experimental conditions under steady state.

2.4 | Analytics

The collected liquid samples were weighed (60 μg) and dissolved in 1.5 mL acetone containing 700 ppm pentadecane (ex situ internal standard) for analysis by gas chromatography with a flame ionization detector (GC-FID) or a mass spectrometry detector (GC–MS). GC-FID analysis was used to determine the concentrations of benzyl alcohol and benzaldehyde with an HP 5890 Series III system, equipped with a Restek column (Rtx-1791, 60 m × 0.25 mm × 0.25 μm) and helium as the carrier gas. The initial temperature was 60°C, then increased by 15°C/min to the final temperature of 250°C. GC–MS was used to identify benzoic acid by an HP 6890 Series GC system with a Restek column (Rxi-5Sil MS, 30 m × 0.25 mm × 0.25 μm) and an HP 5973 Mass Selective Detector. Helium was used as the carrier gas with a split ratio of 50 and a split flow of 48.2 mL/min. The initial temperature was 50°C, then increased by 10°C/min to the final temperature of 210°C.

2.5 | Definitions

The benzyl alcohol conversion (X_{BnOH}) and the yield of the product i (Y_i) are defined as

$$X_{BnOH} = \left(1 - \frac{C_{BnOH,1}}{C_{BnOH,0}}\right) \times 100\%, \quad (1)$$

$$Y_i = \left(\frac{\xi_i C_{i,1}}{C_{BnOH,0}}\right) \times 100\%. \quad (2)$$

Here, C_{BnOH} and C_i represent the concentrations of benzyl alcohol and product i (i.e., mainly benzaldehyde [BnO] or benzoic acid [BnOOH]), respectively. The subscripts 0 and 1 refer to the microreactor inlet and outlet, respectively. ζ_i is the stoichiometric constant based on benzyl alcohol (equal to 1 for benzaldehyde or benzoic acid).

The average residence time (τ) in the microreactor is defined as

$$\tau = \frac{V_C}{Q_{tot}} = \frac{\frac{\pi}{4} {d_C}^2 L_C}{Q_G + Q_L} \quad (3)$$

Here, V_C is the capillary microreactor volume. Q_G, Q_L, and Q_{tot} (= $Q_G + Q_L$) denote the volumetric flow rates of gas, liquid, and the total gas–liquid mixture in the microreactor, respectively. Q_G (and thus Q_{tot}) was derived based on the (reaction) temperature and average pressure in the microreactor according to the ideal gas law. Q_L was assumed roughly equal to $Q_{L,0}$ since the liquid density did not vary much between ambient and elevated temperature/pressure conditions. The gas–liquid mixture velocity in the microreactor (U_M) is defined as

$$U_M = \frac{Q_{tot}}{\frac{\pi}{4} {d_C}^2} \quad (4)$$

3 | RESULTS AND DISCUSSION

3.1 | Selectivity and oxygen depletion

The selectivity toward benzaldehyde is generally 100% for all experiments performed in microreactors with a benzyl alcohol conversion up to ca. 85% (cf. Figure S1a). This corresponds to the highly selective nature of the reaction as it was previously found that only benzaldehyde, benzoic acid and benzyl acetate (traces) were observed as the products.[8,9] Due to the inhibition by benzyl alcohol (i.e., intercepting radicals that induce the further oxidation of benzaldehyde),[9,10] benzoic acid is only formed when benzyl alcohol is consumed to a great extent (e.g., over 85% conversion). The GC columns used in this work were not the most suitable for the quantitative analysis of benzoic acid due to its acidity; hence, this could not be determined with high accuracy. However, no additional side products (apart from traces of benzyl acetate) were detected via either GC-FID or GC–MS. Although the formation of CO_x (i.e., CO and CO_2) by the over-oxidation of the substrate or the acetic acid solvent has been observed during the liquid phase oxidation of *p*-xylene to TPA,[36] and HMF to DFF/FDCA,[8,13] it was found negligibly low in the oxidation of benzyl alcohol (e.g., 0.05% yield toward CO_x).[8] This was further confirmed by performing experiments at low inlet gas to liquid volumetric flow ratios (expressed as $Q_{G,0}/Q_{L,0}$), where there was a stoichiometric

shortage of oxygen (cf. Figure S1b). Note that $Q_{G,0}$, $Q_{L,0}$, and $Q_{tot,0}$ as shown in Figure S1 and hereafter refer to the respective gas, liquid and total mixture flow rates evaluated at the microreactor inlet temperature (i.e., ca. 20°C) and the applied pressure (i.e., 1 or 5 bar; given that the slug flow pressure drop in the microreactor was found much smaller than this value in most cases, except for a few experiments under 1 bar where L_C was above 5 m). The measured benzaldehyde yield in the microreactor approached its maximum attainable yield at longer residence time values, indicating the consumption of all available oxygen in the reaction to form benzaldehyde and the negligibly low occurrence of over-oxidation or burning of solvent and substrate.

3.2 | Absence of mass transfer limitations at low temperatures

To identify whether and when the reaction is limited by mass transfer in the current microreactor system (for the purpose of evaluating the microreactor application potential), experiments were performed under slug flow by varying the flow rate and using capillaries of different lengths and inner diameters (as exemplified in Figure 2), without adjusting variables that may influence kinetics (i.e., temperature, partial oxygen pressure, catalyst, and initial substrate concentrations). The corresponding gas–liquid slug flow photographs are shown in Figure 3.

The gas and liquid flow rates, or more specifically the superficial gas and liquid velocities (j_G and j_L) and the resulted bubble velocity (U_B), have a significant influence on the liquid-side mass transfer coefficient (k_L) in slug flow microreactors.[22,37,38] Figure 2a reveals that at 90°C and 1 bar, the measured benzaldehyde yield was not affected by the total mixture flow rate (with $Q_{G,0}/Q_{L,0}$ being fixed) and only influenced by the residence time. This strongly indicates that the reaction is not limited by mass transfer under these conditions, since a variation of k_L did not change the rate of product formation (and the reactant consumption). The absence of mass transfer limitations was further confirmed by experiments in microreactors of different inner diameters (Figure 2b). Here, the lengths of microreactors were adjusted such that the microreactor volume was equal, meaning that the residence time was fixed given unchanged phasic flow rates. Accordingly, j_G and j_L (and the corresponding U_B) were considerably higher in the smaller-diameter microreactors, resulting in an increased k_L.[39,40] Furthermore, gas–liquid slug flow in smaller-diameter microreactors tends to provide higher interfacial area (a) values for a given $Q_{G,0}/Q_{L,0}$. Thus, the results of Figure 2b imply that the measured benzaldehyde yield was affected by neither k_L nor a. This proves that the benzyl alcohol oxidation under these conditions in microreactors was fully controlled by kinetics.

3.3 | Wetted and dewetted slug flows

Two different slug flow patterns were observed in the experiments described above (Figure 3). At relatively high mixture velocities (U_M; cf. Equation (4)), the rear end cap of bubbles resembles more like a hemispherical or hemi-ellipsoidal shape (Figure 3b–d), whereas the flattening of the rear end cap was observed at relatively low mixture velocities (Figure 3a,) implying the partial dewetting of the liquid film between the bubble and the microreactor wall.

Dewetting is the formation of dry spots caused by rupture of the liquid film and is typically observed at low flow rates under which the film thickness becomes very thin (the flow pattern named here as

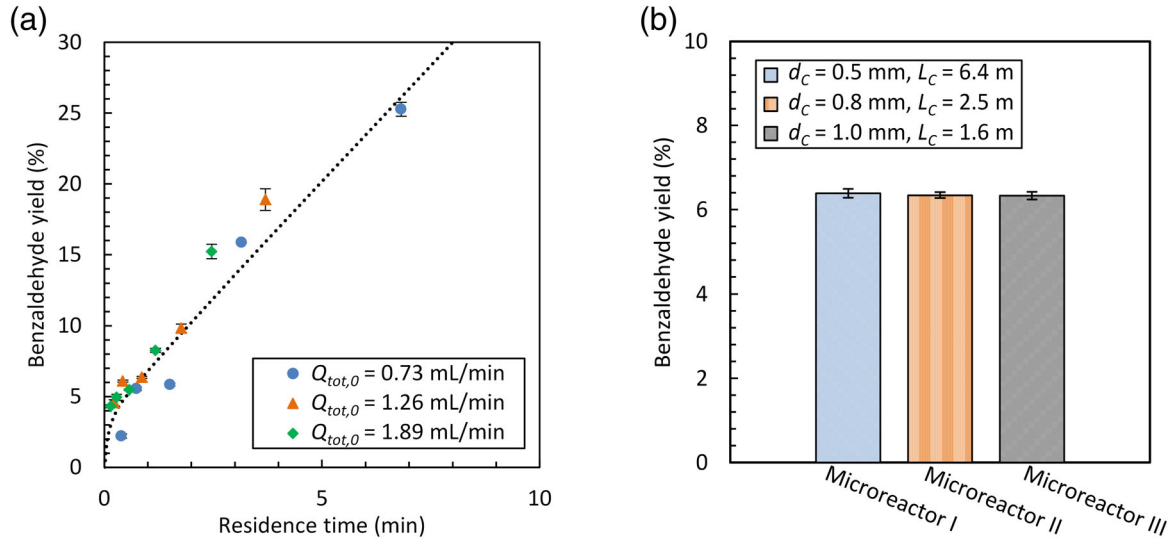

FIGURE 2 (a) Influence of the total mixture flow rate ($Q_{tot,0}$) on the measured benzaldehyde yield at different residence times in the microreactor (d_C = 0.8 mm). For a given $Q_{tot,0}$, the residence time was adjusted by varying the microreactor length (L_C = 0.675–10 m). (b) Measured benzaldehyde yield in microreactors with different inner diameters ($Q_{tot,0}$ = 1.26 mL/min, $\tau \approx 50$ s). Other conditions: 90°C, 1 bar air, $Q_{G,0}/Q_{L,0}$ = 5, $C_{BnOH,0}$ = 185 mM, C_{Co} = 30 mM. Line in (a) is for illustrative purpose only. Error bars shown here and in the following figures were determined by performing experiments at least in duplicate [Color figure can be viewed at wileyonlinelibrary.com]

FIGURE 3 Pictures of the gas–liquid slug flow patterns at the microreactor outlet for the experiments depicted in Figure 2. Other conditions: 90°C, 1 bar air, $Q_{G,0}/Q_{L,0}$ = 5, $C_{BnOH,0}$ = 185 mM, C_{Co} = 30 mM. Flow direction is from left to right [Color figure can be viewed at wileyonlinelibrary.com]

the dewetted slug flow).[30-32] Under fully wetted liquid film conditions for slug flow in a microchannel (named here as the wetted slug flow), the liquid film thickness (δ) can be described as[41]

$$\frac{\delta}{d_C} = \frac{0.66Ca^{\frac{2}{3}}}{1+3.33Ca^{\frac{2}{3}}} \quad (5)$$

where the capillary number Ca is described by

$$Ca = \frac{\mu_L U_B}{\gamma} \quad (6)$$

In Equation (6), μ_L is the liquid viscosity and γ the gas–liquid surface tension. U_B is roughly equal to U_M given very small Ca values (5×10^{-4} to 3.2×10^{-3}) and thus very thin film thickness involved.[40] For a slug flow microreactor, a critical wetting velocity, U_{CW} (i.e., a minimum velocity beyond which the bubble body is completely surrounded by a liquid film), exists depending on the inlet geometry, wall wettability and fluid properties.[30] The contact angle (θ) of a liquid on the microreactor wall determines below which bubble velocity dewetting occurs for a certain fluid pair. For gas–liquid type flows, U_{CW} is proportional to θ^3.[42,43]

$$U_{CW} = \frac{\gamma\theta^3}{6\alpha\mu_L} \quad (7)$$

Here, α is a prefactor depending on the liquid.[43] The static contact angle of acetic acid on PTFE was determined experimentally to be ca. 41° at ambient conditions, which is close to the literature prediction (ca. 49°, cf. section S2).[29] Thus, acetic acid has a good to marginal wetting on PTFE.[44] If the bubble body is fully covered by the liquid film, its rear end cap should have a somewhat hemispherical or hemi-ellipsoidal shape. In the occurrence of dewetting, the shape of the rear end cap should change since gas bubbles directly contact the wall by the formation of (gas–liquid–solid wall) triple lines,[43] thus causing the cap to be flattened or perhaps even curved inward (i.e., of a concave shape).[45]

To identify the flow conditions for a transition from the wetted to dewetted slug flow, flow analyses were performed for air-acetic acid slug flow in a PTFE capillary microreactor (d_C = 0.8 mm) under ambient conditions by varying the inlet gas and liquid flow rates using a similar setup as shown in Figure 1. The existence regions of the corresponding gas–liquid flow patterns are depicted in Figure 4, and the representative flow photographs are given in Figure 5. The wetted slug flow was typically observed at relatively high superficial gas and liquid velocities (or equivalently, relatively high bubble velocities), and the dewetted slug flow occurred at relatively low superficial gas and liquid velocities (Figures 4a and 5a,b). The transition between flow profile when changing the velocity is almost instantaneous. It also seemed that slug-annular flow appeared at relatively high gas to liquid flow ratios at relatively low superficial liquid velocities (Figures 4a and 5c).[21] The transition from the wetted to dewetted slug flow is better revealed based on the existence of such flow patterns as a function of the normalized bubble length (L_B/d_C) and the bubble velocity (Figure 4b). From the transition line in the figure, the critical wetting velocity (U_{CW}) can be estimated at a given bubble length (or alternatively, a given gas-to-liquid flow ratio) for air-acetic acid flow in the PTFE microreactor. Under the gas-to-liquid flow ratio mostly used in this work ($Q_{G,0}/Q_{L,0}$ = 5) for benzyl alcohol oxidation in PTFE microreactors (d_C = 0.8 mm), L_B/d_C was ca. 5.5–6.5 which corresponds to U_{CW} of 30–40 mm/s (Ca = 0.8×10^{-3} to 1.0×10^{-3}) according to Figure 4b. For air-water flow in glass/silica square microchannels (d_C = 0.5 mm), a U_{CW} of 7 mm/s (Ca = 9.61×10^{-5}) was found for gas to liquid flow ratios between 0.4 and 4.[43] Despite that the film thickness is higher for acetic acid at a given bubble velocity (due to the higher Ca given the lower surface tension of air with acetic acid than that with water[46]), U_{CW} for the air-acetic acid system is probably higher due to the higher contact angle of acetic acid on PTFE (41°) compared with water on glass/silica (8–18°),[43] as inferred qualitatively in Equation (7).

For longer bubbles (e.g., L_B/d_C > 7; observed at higher $Q_{G,0}/Q_{L,0}$ values), U_{CW} was found to be higher (Figure 4b). It appears that the rupture of the lubricating liquid film occurs for a given bubble velocity

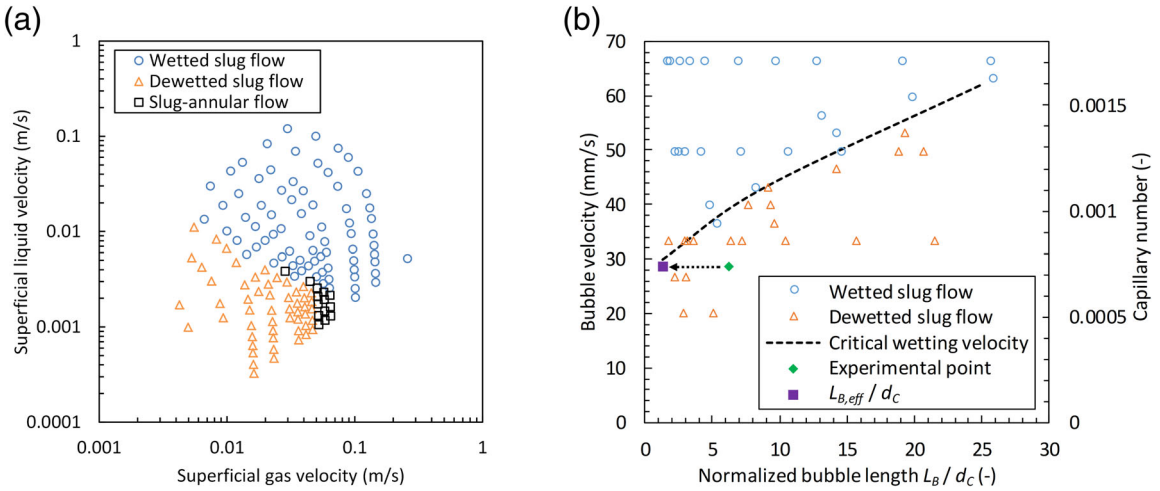

FIGURE 4 Influence of (a) the gas and liquid superficial velocities and (b) normalized bubble length (L_B/d_C), bubble velocity and capillary number on the air-acetic acid flow pattern in a PTFE microreactor (d_C = 0.8 mm, L_C = 1.0 m) at ambient conditions. Line in (b) indicates the estimated critical wetting velocity (U_{CW}). The experimental point and the point related to the predicted normalized effective bubble length ($L_{B,\text{eff}}/d_C$) in (b) correspond to the benzyl alcohol oxidation reaction under the dewetted slug flow at elevated temperature conditions (150°C and 1 bar), where mass transfer limitations were observed (i.e., U_M = 28.6 mm/s and $L_B/d_C \approx 6.2$; vide infra) [Color figure can be viewed at wileyonlinelibrary.com]

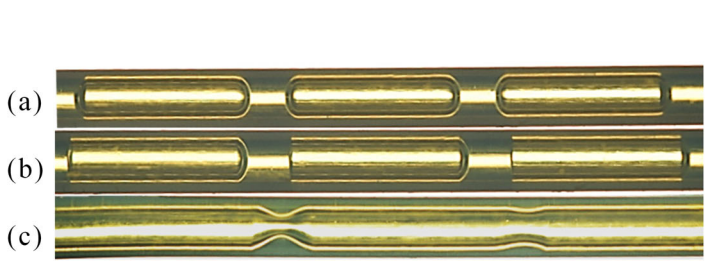

	Q_{tot} (mL/min)	j_G (mm/s)	j_L (mm/s)	Q_G / Q_L (-)
(a)	2.4	66.3	13.3	5
(b)	0.6	16.6	3.3	5
(c)	0.95	30.3	1.2	25

FIGURE 5 Air-acetic acid flow patterns observed in the PTFE microreactor (d_C = 0.8 mm, L_C = 1.0 m) at ambient conditions. (a) Wetted slug flow ($U_B \approx U_M$ = 79.6 mm/s, L_B/d_C = 5.9). (b) Dewetted slug flow ($U_B \approx U_M$ = 19.9 mm/s, L_B/d_C = 5.8). (c) Slug-annular flow (U_M = 31.5 mm/s). Flow direction is from left to right [Color figure can be viewed at wileyonlinelibrary.com]

when the bubble exceeds a certain length.[47] The increase in the film length for longer bubbles causes film thinning to a critical amplitude, inducing its local rupture. The resulting dry spots then rapidly expand to initiate a local drop, rivulet or slug-annular flow regime.[48,49] According to Equations (5)–(7), there is a certain film thickness corresponding to the value of U_{CW}. In other words, it can be stated that dewetting occurs when the film thickness becomes too thin to maintain a complete film for a bubble of a certain length. Thus, there is a maximum bubble length below which a complete wetting is maintained for a given film thickness (corresponding to U_{CW}), as shown in Figure 4b.

It has to be noted that under reactive conditions, the increase of temperature and pressure, and the presence of substrates, products and catalyst in the liquid phase, may affect the fluid physical properties (e.g., viscosity and surface tension) and with that, the contact angle of the liquid on the PTFE microreactor wall and the value of the prefactor (α; Equation (7)). Furthermore, a temperature increase elongates the bubble (i.e., by gas phase expansion), which may also affect U_{CW} (Figure 4b). Hence, U_{CW} under reactive conditions could deviate from values found in the cold flow measurements shown in Figure 4 to some extent. However, the latter results are expected to be largely valid as a first approximation.

The fact that the benzyl alcohol conversion and benzaldehyde yield were not affected by operating under a wetted or dewetted slug flow under the reaction conditions as described in Figure 2a, further proves the absence of mass transfer limitations therein since there is less interfacial area for mass transfer in the dewetted slug flow due to the film rupture than that in the wetted slug flow. More detailed discussion will be provided hereafter.

3.4 | Determination of kinetic parameters at low temperatures

Kinetic studies on the homogeneous Co/Mn/Br catalyzed aerobic oxidation of benzyl alcohol in acetic acid have not been widely examined to this date.[9] Experiments were thus performed within the previously

identified kinetic regime ($T \leq 90°C$, 1 bar air) to determine the kinetic parameters (i.e., the reaction order, activation energy and pre-exponential factor according to the Arrhenius equation). Experiments at 70°C were performed under a dewetted slug flow in order to achieve a sufficiently long residence time (and thus an appreciable benzaldehyde yield). Given that under the same flow conditions the mass transfer rate was not limiting at 90°C and this is not considerably affected by temperature (in contrary to the kinetic rate), it is reasonable to assume that these experiments were also in the kinetic regime.

The cobalt (or catalyst) concentration (C_{Co}) was varied without changing the catalyst composition (Co/Mn/Br = 1/1/3.3 molar ratio). The benzaldehyde yield at a given residence time increased for higher catalyst concentrations (i.e., C_{Co} = 2–30 mM) (Figure 6a). Further increasing the catalyst concentration to 45 mM did not improve the benzaldehyde yield. In the metal bromide catalyzed oxidation of hydrocarbons in general, the reaction rate actually decreased slightly at high catalyst concentrations,[4] which might explain the slightly higher benzaldehyde yield for C_{Co} = 30 mM compared to C_{Co} = 45 mM. At low catalyst concentrations (C_{Co} of ca. 10 mM and below), the reaction was reported of second order in cobalt concentration.[50,51] Hence, for the other experiments in this work, an excessive amount of catalyst was used (C_{Co} = 30 mM) to exclude its influence on kinetics. For the influence of catalyst composition and concentration on the kinetics and reaction mechanism we refer to other works.[7,9] There is no considerable difference in the measured benzaldehyde yield when changing the inlet benzyl alcohol concentration for a given residence time in the microreactor (Figure 6b). Since the benzyl alcohol conversion for these experiments was roughly equal to the benzaldehyde yield (cf. section S1), this was also not affected by the inlet benzyl alcohol concentration. Thus, the reaction is considered first order in benzyl alcohol, which is consistent with the reported kinetic studies on the oxidation of *p*-xylene to terephthalic acid using metal bromide catalysts in acetic acid.[52]

The influence of partial oxygen pressure (p_{O_2}) on the benzaldehyde yield was investigated by performing the reaction at 1 bar using air ($p_{O_2} \approx 0.21$ bar) or pure oxygen (p_{O_2} = 1 bar) as the gas phase in the microreactor (Figure 6c,d). The benzaldehyde yield at a given residence time was practically equal in both cases under otherwise the same reaction conditions (Figure 6c), indicating that the reaction rate is not affected by p_{O_2} and thus zero order in oxygen. This zero order has been reported for the aerobic Co/Mn/Br catalyzed oxidation of *p*-xylene.[52] Furthermore, this is an additional proof that the reaction rate under the involved conditions was not affected by mass transfer of oxygen, given a considerable increase of p_{O_2} when using pure O_2. Interestingly, Figure 6d shows that an increase in the gas to liquid volumetric flow ratio (especially when $Q_{G,0}/Q_{L,0} > 5$) tended to give a higher benzaldehyde yield albeit a fixed total flow rate or almost constant average residence time (calculated using Equation (3)). Since the reaction was performed in the kinetically limited regime, an increase in the benzaldehyde yield is probably due to an increase of the effective liquid-phase residence time.

Under a (wetted) slug flow, the liquid film is almost at rest when the bubble passes by,[40] after which it is shed into the trailing slug (a fully developed laminar flow velocity profile prevails in the slug center provided that it is not too short).[53] At a much increased gas-to-liquid volumetric flow ratio (e.g., at $Q_{G,0}/Q_{L,0}$ = 10 or 20; Figure 6d), the liquid film volume as compared to the slug volume in a unit cell is relatively high (due to a shorter slug and longer liquid film). Since the liquid film could experience a longer actual residence time than the slug body (or than that calculated with Equation (3)), under such circumstances, this would in effect contribute more significantly to an overall increased yield. To further elucidate this, the local residence time distribution in the liquid slug and film especially at large gas–liquid flow ratios needs to be well investigated,[54] and their influence on the current reaction performance needs to be made clearer in our future studies. The kinetic studies in this work are based on a low gas to liquid volumetric flow ratio ($Q_{G,0}/Q_{L,0}$ = 5). Under such conditions, the use of the average residence time is expected sufficient for kinetic parameter estimation (Figure 6d).

From the derived reaction orders (first order in benzyl alcohol and zero order in oxygen), the rate of benzyl alcohol consumption ($-r_{BnOH}$) is simply written as

$$-r_{BnOH} = kC_{BnOH} \tag{8}$$

where k is the pseudo-first order kinetic constant. Equation (8) is valid under the conditions that there is a sufficient oxygen supply and an excessive amount of catalyst available so that this no longer affects the reaction rate. When the reaction rate is only controlled by kinetics, there is according to the mole balance in the microreactor that,

$$\frac{Q_L dC_{BnOH}}{dV_L} = -kC_{BnOH} \tag{9}$$

Here, V_L is the liquid volume in the microreactor. In slug flow at low velocities (i.e., very small Ca values), the liquid film volume is almost negligible and $U_M \approx U_B$.[40] In addition, the pressure drop over the microreactor is negligibly small for most experiments (compared to the absolute pressure applied) and the gas molar flow rate decrease due to the depletion of O_2 is generally insignificant (maximum ca. 10.5% decrease for such kinetic experiments; cf. section S1). Hence, as a first approximation, the gas volumetric flow rate was assumed constant and the average residence time in the microreactor is roughly described as $\tau \approx V_L/Q_L$. By combining Equations (1) and (9) and integrating throughout the microreactor, the benzyl alcohol conversion is described as

$$X_{BnOH} = \left(1 - e^{-\frac{kV_L}{Q_L}}\right) \times 100\% = \left(1 - e^{-k\tau}\right) \times 100\% \tag{10}$$

By performing experiments in the kinetic regime without significant O_2 consumption, k values were obtained at 70 and 90°C, from which the activation energy (E_a = 92.6 kJ/mol) was determined with the Arrhenius equation (cf. section S3 for more details). The value for

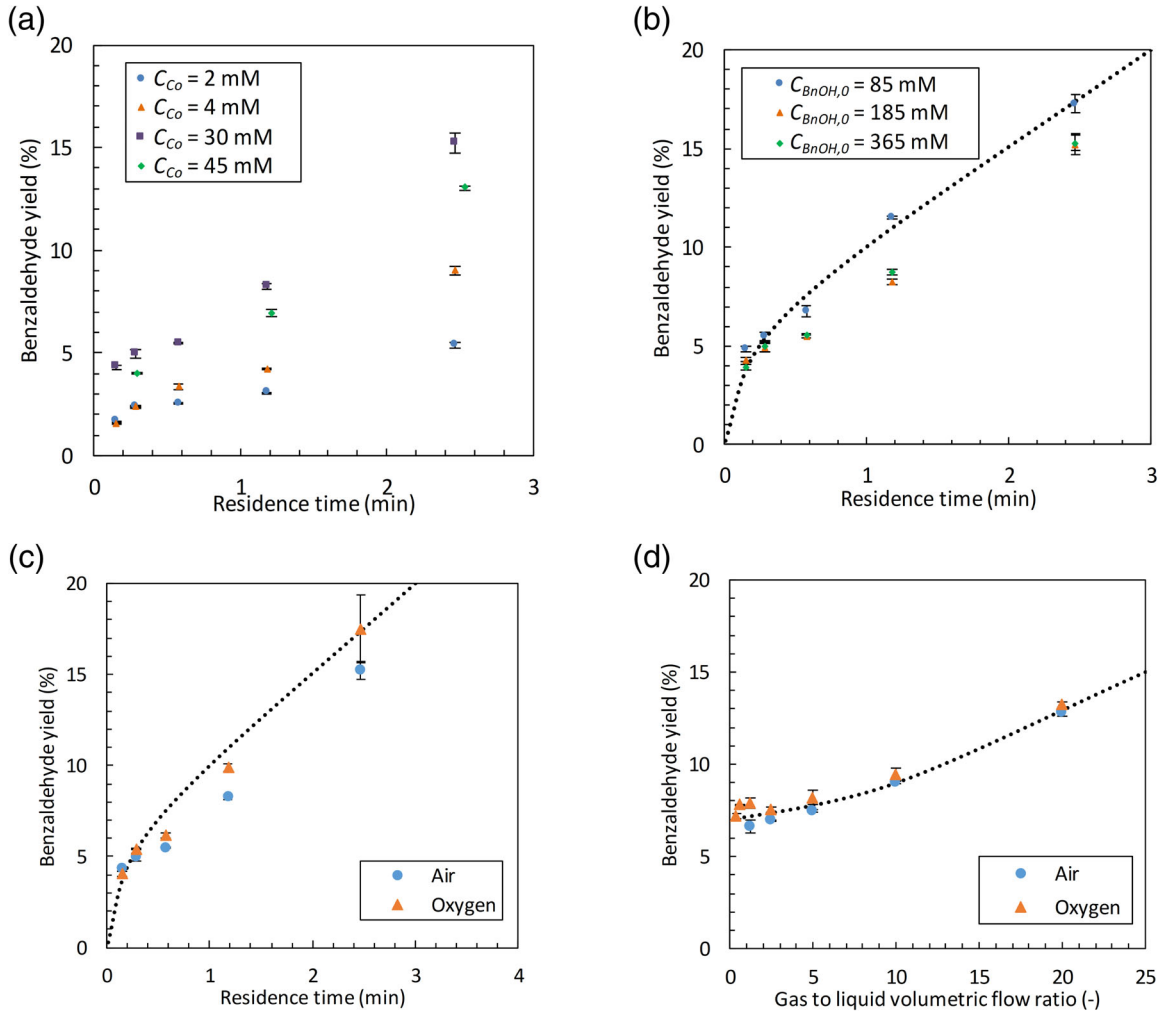

FIGURE 6 Measured benzaldehyde yield in the microreactor as a function of (a–c) the residence time at varying conditions and (d) the inlet gas to liquid volumetric flow ratio ($Q_{G,0}/Q_{L,0}$; where $Q_{tot,0}$ = 2.30 mL/min, L_C = 5 m and $\tau \approx 1$ min). In (a), the catalyst concentration was changed and $C_{BnOH,0}$ = 179–185 mM. In (b), the inlet benzyl alcohol concentration was changed. Air is the gas phase in (a) and (b). Air and pure oxygen were both used as the oxidant in (c) and (d). Conditions (unless stated otherwise): 90°C, 1 bar, d_C = 0.8 mm, $C_{BnOH,0}$ = 185 mM and C_{Co} = 30 mM. The residence time in (a–c) was adjusted by varying the microreactor length (L_C = 0.675–10 m), without changing the flow rate ($Q_{tot,0}$ = 1.89 mL/min, $Q_{G,0}/Q_{L,0}$ = 5). Lines in (b–d) are for illustrative purposes [Color figure can be viewed at wileyonlinelibrary.com]

E_a is some what higher than those reported for the benzyl alcohol oxidation using a cobalt oxide catalyst in toluene (46.2 kJ/mol), or tetrabutylphosphonium and tetrabutylammonium bromide as phase transfer catalysts in benzene (29–30 kJ/mol).[55,56] The estimated k value at 75°C (2.26×10^{-4} s^{-1}) is about half of that for the same reaction with a Co/Mn/Br/Zr catalyst in acetic acid (4.04×10^{-4} s^{-1}), probably due to the enhanced catalytic activity by zirconium present in the latter case.[8]

3.5 | Reaction and mass transfer characteristics at high temperatures

To speed up the reaction rate, the benzyl alcohol oxidation reaction was performed in microreactors at elevated temperatures (90–150°C). To prevent evaporation of the acetic acid solvent (having a boiling point of 118°C under atmospheric pressure) and to increase the oxygen availability, a slightly higher pressure (air at 5 bar) was used (Figure 1).

3.5.1 | Influence of reaction temperature

At 90°C and 5 bar, the benzaldehyde yield was 4.2% at a residence time of ca. 30 s (Figure 7), which is approximately equal to that at atmospheric pressure under otherwise similar conditions (Figure 2a). This further confirms that the reaction is independent of the partial oxygen pressure according to the kinetics. At 130°C and the same residence time, a benzaldehyde yield of 59.9% was obtained. The benzyl alcohol conversion is 99.5% at 150°C with the benzaldehyde yield

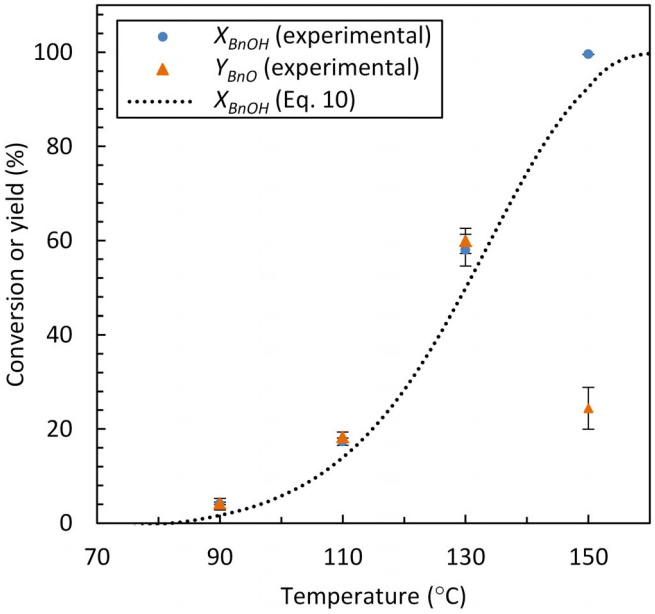

FIGURE 7 Influence of the reaction temperature on the measured benzyl alcohol conversion and benzaldehyde yield in the microreactor operated under a wetted slug flow. The prediction according to Equation (10) is shown for comparison. Other conditions: 5 bar air, d_C = 0.8 mm, L_C = 2.5 m, $C_{BnOH,0}$ = 174 mM, C_{Co} = 30 mM, $Q_{tot,0}$ = 1.89 mL/min, U_M = 75.1–85.8 mm/s, $Q_{G,0}/Q_{L,0}$ = 5, L_B/d_C = 5.5–6.5, τ = 29–34 s [Color figure can be viewed at wileyonlinelibrary.com]

declining to 24.4% due to its further oxidation to benzoic acid. The measured benzyl alcohol concentration is in line with the kinetic model (Equation (10)) for temperatures (at least) up to 150°C when operated under a wetted slug flow (Figure 7), indicating the presence of a kinetically limited regime under the involved flow conditions (d_C = 0.8 mm, $Q_{tot,0}$ = 1.89 ml/min, $Q_{G,0}/Q_{L,0}$ = 5). It should be noted that $Q_{G,0}/Q_{L,0}$ = 5 was chosen herein to ensure a sufficient oxygen amount in the gas for the benzaldehyde formation and a fast mass transfer rate under a wetted slug flow (with the appearance of a complete liquid film) for the reaction to run under kinetic control. This choice is based on experiments at various flow ratios under 150°C and wetted slug flows in the microreactor (cf. section S4 for more details).

3.5.2 | Influence of wetted and dewetted slug flows

To further elucidate the influence of the slug flow profile on the reaction performance, experiments were conducted under wetted and dewetted slug flows in the microreactor at 150°C and 5 bar under the flow ratio ($Q_{G,0}/Q_{L,0}$) of 5 (Figure 8). Under the wetted slug flow, over 80% benzyl alcohol conversion and benzaldehyde yield were obtained in only 18 s (Figure 8a). At a higher benzyl alcohol conversion, the benzaldehyde yield dropped due to its further oxidation to benzoic acid. A difference in the reaction performance was observed between the wetted and dewetted slug flows (realized via changing the flow rate for a given residence time). The reaction rate is considerably lower for the dewetted slug flow (Figure 8b), where it took more than twice as long to obtain the same benzyl alcohol conversion or benzaldehyde yield as compared to the wetted slug flow case (Figure 8a). Furthermore, in the wetted slug flow experiments, the measured benzyl alcohol conversion for different residence times is described well by the kinetic model (Equation (10); Figure 8a), indicating that the reaction rate is not affected by mass transfer. For the dewetted slug flow (Figure 8b), however, the kinetic model overestimated the measured benzyl alcohol conversion until a full conversion was reached, indicating mass transfer limitations. This limitation is likely due to a reduction in the effective interfacial area caused by the (partial) dewetting of the liquid film (vide infra).

3.5.3 | Interfacial area in slug flow

The interfacial area (a) contributing to mass transfer in the wetted slug flow through microreactors can be divided into the film and cap areas (Figure 9). The film area (a_{film}) is estimated by considering the bubble body as a cylinder with a bubble diameter of d_B and a length equal to the film length (L_{film}). Since the film thickness is negligibly small given the low U_B (or Ca) values in this study, it is assumed that $d_B \approx d_C$. The cap area (a_{cap}) is estimated by considering the end caps as hemispheres with a radius of L_{cap} approximately equal to $d_C/2$. Thus, there is for the wetted slug flow

$$a = a_{cap} + a_{film} \approx \frac{4(d_C + L_{film})}{d_C(L_B + L_S)} \tag{11}$$

Here, L_B and L_S are the respective bubble and slug lengths that were measured from the pictures taken at the microreactor outlet for each experiment performed (Figure 9).

For the dewetted slug flow, the film rupture around the bubble body did not induce a complete disappearance of the film area. When there are ruptured liquid droplets or rivulets adhered to the wall and/or when part of the liquid film is still intact (e.g., in the front part of the bubble body), these still contribute to the interfacial area and thus mass transfer. Since the exact geometry of the film in the dewetted slug flow could not be precisely determined with the current flow visualization method, an effective film length ($L_{film,eff}$) was estimated. $L_{film,eff}$ is a hypothetical film length corresponding to the effective film area contributing to mass transfer. The value of $L_{film,eff}$ is assumed approximately equal to the film length corresponding to the maximum bubble length when the bubble is still fully wetted at this U_B, which can be inferred from the relation between L_B/d_C and U_{CW} (=U_B herein) (Figure 4b). Furthermore, the rear end cap area for the dewetted slug flow (possibly of a flat or concave shape) contributes to mass transfer. For a first approximation, this end cap is assumed to have the same area as that in a wetted slug flow (i.e., a_{cap}

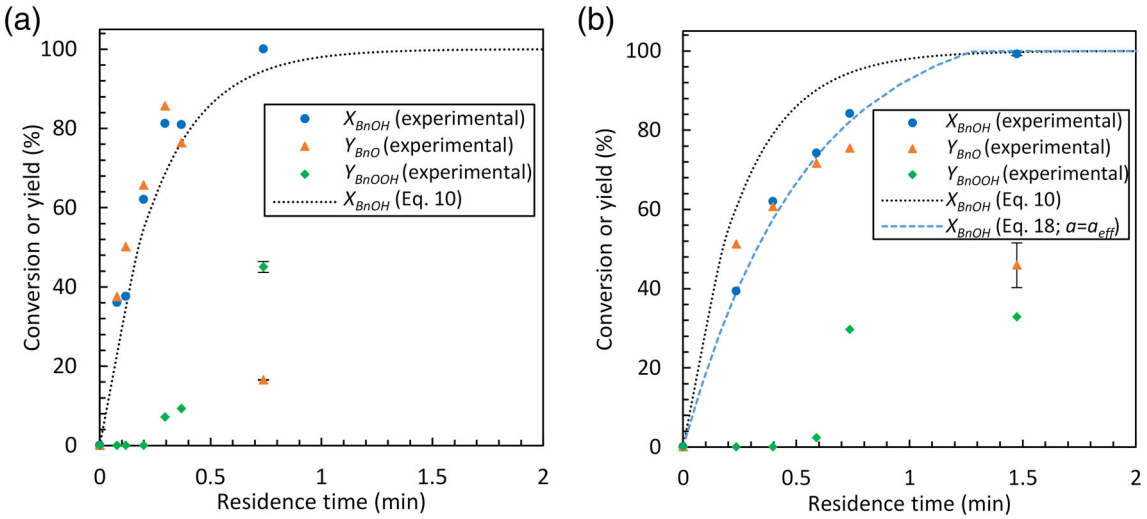

FIGURE 8 Influence of the residence time on the measured benzyl alcohol conversion and product yield for (a) the wetted slug flow ($Q_{tot,0}$ = 1.26 mL/min, $U_M \approx$ 57.2 mm/s) and (b) dewetted slug flow ($Q_{tot,0}$ = 0.63 mL/min, $U_M \approx$ 28.6 mm/s). A comparison with the kinetic model (Equation (10)) or the mass transfer model (Equation (18)) is also provided. Other conditions: 150°C, 5 bar air. d_C = 0.8 mm, $C_{BnOH,0}$ = 174 mM, C_{Co} = 30 mM, $Q_{G,0}/Q_{L,0}$ = 5, L_B/d_C = 5.5–6.5. The residence time was adjusted by varying the microreactor length (L_C = 0.4–2.5 m). Error bars are shown for some data points collected at relatively longer residence times from experiments performed at least in duplicate [Color figure can be viewed at wileyonlinelibrary.com]

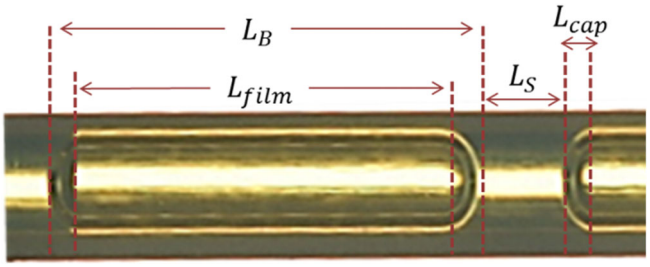

FIGURE 9 Bubble and slug dimensions for a wetted gas–liquid slug flow ($Q_{G,0}/Q_{L,0}$ = 5) in the PTFE microreactor (d_C = 0.8 mm) [Color figure can be viewed at wileyonlinelibrary.com]

is not significantly affected by dewetting). Thus, the effective interfacial area (a_{eff}) in the dewetted slug flow is defined similarly to Equation (11) as

$$a_{eff} \approx \frac{4(d_C + L_{film,eff})}{d_C(L_B + L_S)} \tag{12}$$

3.5.4 | Mass transfer model in the dewetted slug flow

Under mass transfer limited conditions, that is, under a dewetted slug flow ($Q_{G,0}/Q_{L,0}$ = 5) at 150°C and 5 bar air as depicted in Figure 8b, there is according to the mole balance in the microreactor

$$\frac{Q_L dC_{BnOH}}{dV_C} = -\xi_{BnOH} J_{O_2} a \tag{13}$$

The stoichiometric constant of benzyl alcohol (ζ_{BnOH}) is 2, as one oxygen molecule reacts with two benzyl alcohol molecules to form benzaldehyde and there was no side product formation. This equation applies when all converted benzyl alcohol is transformed to benzaldehyde without considerable benzoic acid formation (i.e., when X_{BnOH} < ca. 85%). The oxygen mass transfer flux (J_{O_2}) is described as

$$J_{O_2} = k_L E (C_{O_2,I,L} - C_{O_2,B,L}) \tag{14}$$

where E is the enhancement factor by chemical reaction. $C_{O_2,I,L}$ and $C_{O_2,B,L}$ are the liquid-phase oxygen concentrations at the interface and in the bulk, respectively. The oxygen concentration in the gas phase (air) is assumed constant in the microreactor given no significant oxygen depletion (i.e., a maximum of 30% oxygen consumption at 80% benzyl alcohol conversion for $C_{BnOH,0}$ = 174 mM, $Q_{G,0}/Q_{L,0}$ = 5 and air at 5 bar; equations (S1) and (S2)). Then, the gas phase mass transfer resistance is neglected, and it follows that

$$C_{O_2,I,L} = HC_{O_2,I,G} = HC_{O_2,B,G} \tag{15}$$

where $C_{O_2,I,G}$ and $C_{O_2,B,G}$ are the gas-phase oxygen concentrations at the interface and in the bulk, respectively, and H is the Henry coefficient accounting for the solubility of oxygen in the acetic acid solvent.[57] $C_{O_2,I,L}$ is thus assumed constant throughout the microreactor.

The liquid-side mass transfer coefficient, k_L, was calculated with the empirical correlation proposed in the literature[37] (cf. sections S5 and S6 for the calculation details). Then, the Hatta numbers (Ha) for

the dewetted slug flow conditions relevant to Figure 8b could be calculated (cf. equation (S19)). Since *Ha* was roughly much larger than E_∞ throughout the microreactor, the reaction was simply considered instantaneous (cf. section S7 for more details). That is, the enhancement factor equals the infinite enhancement factor (E_∞) defined as

$$E_\infty = 1 + \frac{C_{\mathrm{BnOH}}}{\xi_{\mathrm{BnOH}} C_{\mathrm{O_2},l,L}} \left(\frac{D_{\mathrm{BnOH}}}{D_{\mathrm{O_2}}} \right) \tag{16}$$

where $D_{\mathrm{O_2}}$ and D_{BnOH} are the respective diffusion coefficients of oxygen and benzyl alcohol in acetic acid (cf. section S6.5 for detailed calculations).

Under such circumstances, $C_{\mathrm{O_2},B,L} = 0$. A combination of Equations (13), (14), and (16) yields

$$\frac{Q_L dC_{\mathrm{BnOH}}}{dV_C} = -\xi_{\mathrm{BnOH}} k_L a \left(1 + \frac{C_{\mathrm{BnOH}}}{\xi_{\mathrm{BnOH}} C_{\mathrm{O_2},l,L}} \left(\frac{D_{\mathrm{BnOH}}}{D_{\mathrm{O_2}}} \right) \right) C_{\mathrm{O_2},l,L} \tag{17}$$

The benzyl alcohol conversion in the microreactor was then obtained based on an integration of Equation (17) between the microreactor inlet and outlet to obtain C_{BnOH}, in combination with Equation (1) (cf. section S7 or more details):

$$X_{\mathrm{BnOH}} = \left(1 - \left(1 + \frac{\xi_{\mathrm{BnOH}} C_{\mathrm{O_2},l,L}}{C_{\mathrm{BnOH},0}} \left(\frac{D_{\mathrm{O_2}}}{D_{\mathrm{BnOH}}} \right) \right) e^{-\frac{k_L a}{Q_L} \left(\frac{D_{\mathrm{BnOH}}}{D_{\mathrm{O_2}}} \right) V_C} + \frac{\xi_{\mathrm{BnOH}} C_{\mathrm{O_2},l,L}}{C_{\mathrm{BnOH},0}} \left(\frac{D_{\mathrm{O_2}}}{D_{\mathrm{BnOH}}} \right) \right) \times 100\% \tag{18}$$

Note that for the dewetted slug flow, the effective interfacial area should be used given the presence of an incomplete liquid film (i.e., $a = a_{\mathrm{eff}}$ in Equation (18)). From Figure 8b, it is seen that the measured benzyl alcohol conversion under the dewetted slug flow can be well described by Equation (18) with a fitted value of a_{eff} at 680 m^2/m^3. From this a_{eff} value, the effective film length was then estimated with Equation (12) ($L_{\mathrm{film,eff}} \approx 0.23$ mm) and thus the corresponding effective bubble length was calculated ($L_{\mathrm{B,eff}} \approx L_{\mathrm{film,eff}} + 2L_{\mathrm{cap}} \approx 1.02$ mm; considering $L_{\mathrm{cap}} \approx d_C/2$) for the dewetted slug flow conditions relevant to Figure 8b. This $L_{\mathrm{B,eff}}$ describes the hypothetical length of a bubble that is fully covered by a complete film corresponding to a wetted slug flow with $a = a_{\mathrm{eff}}$ under the dewetted slug flow for the same U_B. The normalized effective bubble length was then calculated as $L_{\mathrm{B,eff}}/d_C \approx 1.28$ for the dewetted slug flow experiments presented in Figure 8b (at $U_M \approx U_B \approx 28.6$ mm/s). As shown in Figure 4b, for the same U_B value, the maximum normalized bubble length to maintain the wetted slug flow (indicated from the critical wetting velocity line) is more or less the same as 1.28. This justifies the use of Equation (18) for reaction performance prediction under the dewetted slug flow, and the use of $L_{\mathrm{film,eff}}$ for the estimation of a_{eff} (and vice versa) under such flow conditions (Equation (12)).

The value of a_{eff} lies between the value of a for a wetted slug flow with the same bubble and slug lengths ($a \approx 3{,}881$ m^2/m^3 at $Q_{G,0}/Q_{L,0} = 5$; $L_B \approx 4.96$ mm and $L_S \approx 1.43$ mm; Equation (11)) and the interfacial area of the end caps ($a_{\mathrm{cap}} \approx 626$ m^2/m^3; calculated using Equation (12) with $L_{\mathrm{film,eff}} = 0$). This indicates that under the dewetted slug flow, besides the end caps, the film side contributes to mass transfer (e.g., from the partially intact liquid film and/or ruptured liquid droplets adhered to the microreactor wall). Note that this approximation of a_{eff} is based on k_L estimated from the empirical correlation applicable for wetted slug flow profiles (cf. section S5).[37] The actual k_L value may be (slightly) different, which influences the estimated a_{eff}. However, the good prediction performance of Equation (18) (cf. Figure 8b) corroborates that the current approach is reasonable. Dedicated studies are still needed for developing mass transfer correlations for the dewetted slug flow in our ongoing work.

3.5.5 | Microreactor optimization strategy

For an optimal microreactor performance in terms of mass transfer rate, operation under a wetted slug flow is desired as the whole bubble surface is utilized in mass transfer. In such case, dewetting should be avoided by operating at relatively high flow rates/velocities (i.e., above the critical wetting velocity) in the PTFE microreactor (e.g., cf. Figure 4). Accordingly, the use of longer microreactors can be an outcome in order to maintain the required residence time for achieving a desirable conversion or yield. Furthermore, by using a microreactor material with a better solvent wettability (i.e., a low contact angle), the critical wetting velocity decreases (Equation (7)) so that dewetting could be prevented even at lower flow rates. Hence, more hydrophilic microreactor materials (e.g., glass, fused silica or stainless steel) might be more suitable than PTFE for the reaction performed in this work, as the contact angle of acetic acid is lower on these materials (e.g., 4.5° on glass; cf. section S2), which represent a further research direction to explore. However, PTFE has the advantages that it is inert to many solvents, transparent for easy flow monitoring and non-corrosive (e.g., compared with stainless steel). Furthermore, it is more flexible than fused silica and glass, so that the use of long coiled PTFE microreactors is facilitated to achieve sufficiently long residence times for reaction purposes and/or to make a compact reactor module. As such, in some cases, operation under a dewetted slug flow might be inevitable, where a fine tuning of mass transfer is important.

4 | CONCLUSIONS

The homogeneous Co/Mn/Br catalyzed aerobic oxidation of benzyl alcohol to benzaldehyde was performed in PTFE microreactors operated under slug flow using acetic acid as the solvent and air or pure oxygen as the oxidant. Under optimized conditions (150°C and 5 bar air), an 85.6% benzaldehyde yield could be obtained in 18 s. The reaction was highly selective towards benzaldehyde and a further oxidation of benzaldehyde toward benzoic acid only occurred at ca. > 85% benzyl alcohol conversion. Depending on the bubble velocity and length, a wetted or dewetted slug flow was observed, characterized typically by a complete or partially wetting liquid film surrounding the bubble body. The latter flow renders less interfacial area for mass transfer due to the (partial) rupture of the film. Reactions under temperatures up to ca. 90°C were found in the kinetic regime, given no product yield dependence on the flow velocity, (wetted or dewetted) slug flow profile and microreactor diameter. A simplified kinetic expression was thus developed thereof (first order in benzyl alcohol and zero order in oxygen) that well describes the experimental data. Although the kinetic regime can be extended to operation under slightly elevated conditions (150°C and 5 bar air) and a wetted slug flow (at a gas-to-liquid volumetric flow ratio of 5), this did not hold for the dewetted slug flow operation due to mass transfer limitations under similar reaction conditions. A mass transfer model based on an instantaneous reaction regime was proposed, with the additional use of an effective interfacial area responsible for the mass transfer rate decrease in the dewetted slug flow. The developed mass transfer model and other findings in this work are expected to provide additional insights on the aerobic oxidation of benzyl alcohol as well as other substrates in slug flow microreactors using similar catalytic systems.

ACKNOWLEDGMENTS

This work was financially supported by the University of Groningen (startup package in the area of green chemistry and technology for Jun Yue).

ORCID

Jun Yue https://orcid.org/0000-0003-4043-0737

REFERENCES

1. Stahl SS, Alsters PL. *Liquid Phase Aerobic Oxidation Catalysis: Industrial Applications and Academic Perspectives*. Weinheim: Wiley-VCH; 2016.
2. Punniyamurthy T, Velusamy S, Iqbal J. Recent advances in transition metal catalyzed oxidation of organic substrates with molecular oxygen. *Chem Rev*. 2005;105(6):2329-2363.
3. Tomás RAF, Bordado JCM, Gomes JFP. P-xylene oxidation to terephthalic acid: a literature review oriented toward process optimization and development. *Chem Rev*. 2013;113(10):7421-7469.
4. Partenheimer W. Methodology and scope of metal/bromide autoxidation of hydrocarbons. *Catal Today*. 1995;23(2):69-158.
5. Borgaonkar HV, Raverkar SR, Chandalla SB. Liquid phase oxidation of toluene to benzaldehyde by air. *Ind Eng Chem Prod Res Dev*. 1984;23(3):455-458.
6. Kantam ML, Sreekanth P, Rao KK, Kumar TP, Rao BPC, Choudary BM. An improved process for selective liquid-phase air oxidation of toluene. *Catal Lett*. 2002;81(3–4):223-232.
7. Bukharkina TV, Digurov NG. Kinetics of aerobic liquid-phase oxidation of organic compounds. *Org Process Res Dev*. 2004;8(3):320-329.
8. Partenheimer W, Grushin VV. Synthesis of 2,5-diformylfuran and furan-2,5-dicarboxylic acid by catalytic air-oxidation of 5-hydroxymethylfurfural. unexpectedly selective aerobic oxidation of benzyl alcohol to benzaldehyde with metal/bromide catalysts. *Adv Synth Catal*. 2001;343(1):102-111.
9. Partenheimer W. The high yield synthesis of benzaldehydes from benzylic alcohols using homogeneously catalyzed aerobic oxidation in acetic acid. *Adv Synth Catal*. 2006;348(4–5):559-568.
10. Sankar M, Nowicka E, Carter E, et al. The benzaldehyde oxidation paradox explained by the interception of peroxy radical by benzyl alcohol. *Nat Commun*. 2014;5(3332):1-6.
11. Brühne F, Wright E. *Benzaldehyde. Ullman's encyclopedia of industrial chemistry*. Vol 6. Weinheim: Wiley-VCH; 2011:1-13.
12. van Putten RJ, van der Waal JC, de Jong E, Rasrendra CB, Heeres HJ, de Vries JG. Hydroxymethylfurfural, a versatile platform chemical made from renewable resources. *Chem Rev*. 2013;113(3):1499-1597.
13. Zuo X, Venkitasubramanian P, Busch DH, Subramaniam B. Optimization of co/Mn/Br-catalyzed oxidation of 5-hydroxymethylfurfural to enhance 2,5-furandicarboxylic acid yield and minimize substrate burning. *ACS Sustain Chem Eng*. 2016;4(7):3659-3668.
14. Zuo X, Chaudhari AS, Snavely K, et al. Kinetics of homogeneous 5-hydroxymethylfurfural oxidation to 2,5-furandicarboxylic acid with co/Mn/Br catalyst. *AIChE J*. 2017;63(1):162-171.
15. Sajid M, Zhao X, Liu D. Production of 2,5-furandicarboxylic acid (FDCA) from 5-hydroxymethylfurfural (HMF): recent progress focusing on the chemical-catalytic routes. *Green Chem*. 2018;20(24):5427-5453.
16. Partenheimer W. The aerobic oxidative cleavage of lignin to produce hydroxyaromatic benzaldehydes and carboxylic acids via metal/bromide catalysts in acetic acid/water mixtures. *Adv Synth Catal*. 2009;351(3):456-466.
17. Cheng C, Wang J, Shen D, et al. Catalytic oxidation of lignin in solvent systems for production of renewable chemicals: a review. *Polymers*. 2017;9(6):38-50.
18. Hessel V, Angeli P, Gavriilidis A, Löwe H. Gas-liquid and gas-liquid-solid microstructured reactors: contacting principles and applications. *Ind Eng Chem Res*. 2005;44(25):9750-9769.
19. Günther A, Jensen KF. Multiphase microfluidics: from flow characteristics to chemical and materials synthesis. *Lab Chip*. 2006;6(12):1487-1503.
20. Chen G, Yue J, Yuan Q. Gas-liquid microreaction technology: recent developments and future challenges. *Chinese J Chem Eng*. 2008;16(5):663-669.
21. Yue J, Luo L, Gonthier Y, Chen G, Yuan Q. An experimental investigation of gas-liquid two-phase flow in single microchannel contactors. *Chem Eng Sci*. 2008;63(16):4189-4202.
22. Kashid MN, Renken A, Kiwi-Minsker L. Gas-liquid and liquid-liquid mass transfer in microstructured reactors. *Chem Eng Sci*. 2011;66(17):3876-3897.
23. Gemoets HPL, Su Y, Shang M, Hessel V, Luque R, Noël T. Liquid phase oxidation chemistry in continuous-flow microreactors. *Chem Soc Rev*. 2016;45(1):83-117.
24. Gavriilidis A, Constantinou A, Hellgardt K, et al. Aerobic oxidations in flow: opportunities for the fine chemicals and pharmaceuticals industries. *React Chem Eng*. 2016;1(6):595-612.
25. Obermayer D, Balu AM, Romero AA, Goessler W, Luque R, Kappe CO. Nanocatalysis in continuous flow: supported iron oxide nanoparticles for the heterogeneous aerobic oxidation of benzyl alcohol. *Green Chem*. 2013;15(6):1530-1537.

26. Wu G, Constantinou A, Cao E, et al. Continuous heterogeneously catalyzed oxidation of benzyl alcohol using a tube-in-tube membrane microreactor. *Ind Eng Chem Res*. 2015;54(16):4183-4189.
27. Al-Rifai N, Galvanin F, Morad M, et al. Hydrodynamic effects on three phase micro-packed bed reactor performance - gold-palladium catalysed benzyl alcohol oxidation. *Chem Eng Sci*. 2016;149:129-142.
28. Vanoye L, Pablos M, de Bellefon C, Favre-Réguillon A. Gas-liquid segmented flow microfluidics for screening copper/tempo-catalyzed aerobic oxidation of primary alcohols. *Adv Synth Catal*. 2015;357(4):739-746.
29. Kim BS, Harriott P. Critical entry pressure for liquids in hydrophobic membranes. *J Colloid Interface Sci*. 1987;115(1):1-8.
30. Jose BM, Cubaud T. Formation and dynamics of partially wetting droplets in square microchannels. *RSC Adv*. 2014;4(29):14962-14970.
31. Günther A, Jhunjhunwala M, Thalmann M, Schmidt MA, Jensen KF. Micromixing of miscible liquids in segmented gas-liquid flow. *Langmuir*. 2005;21(4):1547-1555.
32. Yue J, Rebrov EV, Schouten JC. Gas-liquid-liquid three-phase flow pattern and pressure drop in a microfluidic chip: similarities with gas-liquid/liquid-liquid flows. *Lab Chip*. 2014;14(9):1632-1649.
33. Hecht K, Fröhlich G, Pfeifer P, Dittmeyer R, Kraushaar-Czarnetzki B. The influence of surface properties on chemical reaction in multiphase flow in capillaries. *Chem Eng J*. 2013;225:837-847.
34. Wang X, Yong Y, Yang C, Mao ZS, Li D. Investigation on pressure drop characteristic and mass transfer performance of gas-liquid flow in micro-channels. *Microfluid Nanofluidics*. 2014;16(1–2):413-423.
35. Oskooei SAK, Sinton D. Partial wetting gas-liquid segmented flow microreactor. *Lab Chip*. 2010;10(13):1732-1734.
36. Partenheimer W. Chemistry of the oxidation of acetic acid during the homogeneous metal-catalyzed aerobic oxidation of alkylaromatic compounds. *Appl Catal Gen*. 2011;409-410:48-54.
37. Yue J, Chen G, Yuan Q, Luo L, Gonthier Y. Hydrodynamics and mass transfer characteristics in gas-liquid flow through a rectangular microchannel. *Chem Eng Sci*. 2007;62(7):2096-2108.
38. Haase S, Murzin DY, Salmi T. Review on hydrodynamics and mass transfer in minichannel wall reactors with gas–liquid Taylor flow. *Chem Eng Res des*. 2016;113:304-329.
39. van Baten JM, Krishna R. CFD simulations of mass transfer from Taylor bubbles rising in circular capillaries. *Chem Eng Sci*. 2004;59(12):2535-2545.
40. Yue J, Luo L, Gonthier Y, Chen G, Yuan Q. An experimental study of air-water Taylor flow and mass transfer inside square microchannels. *Chem Eng Sci*. 2009;64(16):3697-3708.
41. Aussillous P, Quéré D. Quick deposition of a fluid on the wall of a tube. *Phys Fluids*. 2000;12(10):2367-2371.
42. Redon C, Brochard-Wyart F, Rondelez F. Dynamics of dewetting. *Phys Rev Lett*. 1991;66(6):715-718.
43. Cubaud T, Ho CM. Transport of bubbles in square microchannels. *Phys Fluids*. 2004;16(12):4575-4585.
44. Lee CY, Lee SY. Influence of surface wettability on transition of two-phase flow pattern in round mini-channels. *Int J Multiph Flow*. 2008;34(7):706-711.
45. Blake TD. The physics of moving wetting lines. *J Colloid Interface Sci*. 2006;299(1):1-13.
46. Ikeda H, Suzuki A. Wettability effects of plate materials on hydrodynamics in a pulsed perforated-plate extraction column of pulser feeder type. *Ind Eng Chem Res*. 1995;34(11):4110-4117.
47. Wong H, Radke CJ, Morris S. The motion of long bubbles in polygonal capillaries. Part 1. Thin films. *J Fluid Mech*. 1995;292:71-94.
48. Cubaud T, Ulmanella U, Ho CM. Two-phase flow in microchannels with surface modifications. *Fluid Dyn Res*. 2006;38(11):772-786.
49. Borhani N, Agostini B, Thome JR. A novel time strip flow visualisation technique for investigation of intermittent dewetting and dryout in elongated bubble flow in a microchannel evaporator. *Int J Heat Mass Transf*. 2010;53(21–22):4809-4818.
50. Scott EJY, Chester AW. Kinetics of the cobalt-catalyzed autoxidation of toluene in acetic acid. The role of cobalt. *J Phys Chem*. 1972;76(11):1520-1524.
51. Hendriks CF, van Beek HCA, Heertjes PM. The kinetics of the autoxidation of aldehydes in the presence of cobalt(II) and cobalt(III) acetate in acetic acid solution. *Ind Eng Chem Prod Res Dev*. 1978;17(3):260-264.
52. Li M, Niu F, Busch DH, Subramaniam B. Kinetic investigations of p-xylene oxidation to terephthalic acid with a Co/Mn/Br catalyst in a homogeneous liquid phase. *Ind Eng Chem Res*. 2014;53(22):9017-9026.
53. Donaldson AA, Macchi A, Kirpalani DM. Predicting inter-phase mass transfer for idealized Taylor flow: a comparison of numerical frameworks. *Chem Eng Sci*. 2011;66(14):3339-3349.
54. Trachsel F, Günther A, Khan S, Jensen KF. Measurement of residence time distribution in microfluidic systems. *Chem Eng Sci*. 2005;60(21):5729-5737.
55. Bijudas K, Bashpa P, Radhakrishnan Nair TD. Kinetic studies on the selective oxidation of benzyl alcohol and substituted benzyl alcohols in organic medium under phase transfer catalysis. *Bull Chem React Eng Catal*. 2014;9(2):142-147.
56. Ilyas M, Saeed M. Oxidation of benzyl alcohol in liquid phase catalyzed by cobalt oxide. *Int J Chem React Eng*. 2010;8(1).
57. Wu X, Deng Z, Yan J, Zhang Z, Zhang F, Zhang Z. Experimental investigation on the solubility of oxygen in toluene and acetic acid. *Ind Eng Chem Res*. 2014;53(23):9932-9937.

SUPPORTING INFORMATION

Additional supporting information may be found online in the Supporting Information section at the end of this article.

How to cite this article: Hommes A, Disselhorst B, Yue J. Aerobic oxidation of benzyl alcohol in a slug flow microreactor: Influence of liquid film wetting on mass transfer. *AIChE J*. 2020;66:e17005. https://doi.org/10.1002/aic.17005